Molecular Biology of the Cell
Vol. 18, 3169–3179, August 2007

# Rab11A Controls the Biogenesis of Birbeck Granules by Regulating Langerin Recycling and Stability[D]

**Stéphanie Uzan-Gafsou,* Huguette Bausinger,†‡§ Fabienne Proamer,†‡§ Solange Monier,* Dan Lipsker,†‡§ Jean-Pierre Cazenave,‡§‖ Bruno Goud,* Henri de la Salle,†‡§ Daniel Hanau,†‡§ and Jean Salamero***

*Unité Mixte de Recherche 144 Centre National de la Recherche Scientifique-Institut Curie, Laboratoire "Mécanismes Moléculaires du Transport Intracellulaire," Institut Curie, 75248 Paris Cedex 05, France; †U 725 "Biologie des Cellules Dendritiques Humaines" and ‖U 311, Institut National de la Santé et de la Recherche Médicale, F-67065 Strasbourg, France; ‡Université Louis Pasteur, F-67000 Strasbourg, France; and §Etablissement Français du Sang-Alsace, F-67065 Strasbourg, France

Submitted September 5, 2006; Revised April 30, 2007; Accepted May 17, 2007
Monitoring Editor: Sandra Schmid

**The extent to which Rab GTPases, Rab-interacting proteins, and cargo molecules cooperate in the dynamic organization of membrane architecture remains to be clarified. Langerin, a recycling protein accumulating in the Rab11-positive compartments of Langerhans cells, induces the formation of Birbeck granules (BGs), which are membrane subdomains of the endosomal recycling network. We investigated the role of Rab11A and two members of the Rab11 family of interacting proteins, Rip11 and RCP, in Langerin traffic and the biogenesis of BGs. The overexpression of a dominant-negative Rab11A mutant or Rab11A depletion strongly influenced Langerin traffic and stability and the formation of BGs, whereas modulation of other Rab proteins involved in dynamic regulation of the endocytic-recycling pathway had no effect. Impairment of Rab11A function led to a missorting of Langerin to lysosomal compartments, but inhibition of Langerin degradation by chloroquine did not restore the formation of BGs. Loss of RCP, but not of Rip11, also had a modest, but reproducible effect on Langerin stability and BG biogenesis, pointing to a role for Rab11A–RCP complexes in these events. Our results show that Rab11A and Langerin are required for BG biogenesis, and they illustrate the role played by a Rab GTPase in the formation of a specialized subcompartment within the endocytic-recycling system.**

## INTRODUCTION

The endosomal system consists of an interconnected and dynamic network of membranes differing in their cellular distribution, overall morphology, and biochemical composition (Hopkins *et al*., 1990; Pfeffer, 2003). Furthermore, within a given membrane system, the proteins and lipids are unevenly distributed throughout the bilayer, forming organized domains (Pfeffer, 2003). A compartment may therefore be viewed as a unique, dynamic combination of specific domains, coupled both spatially and functionally. There is growing evidence to suggest that members of the Rab GTPase family play a key role in the generation and maintenance of this compartmentalized mosaic of membrane domains (Zerial and McBride, 2001). Such a role has been clearly established for Rabs of the endocytic pathway, such as Rab5, Rab11, Rab4, and Rab9 (Sonnichsen *et al*., 2000; de Renzis *et al*., 2002; Hanna *et al*., 2002; Ganley *et al*., 2004).

In their active GTP-bound state, Rab proteins interact with a multitude of effectors. The clustering of Rab proteins with these effectors in defined membrane domains enables them to regulate the various steps of transport between compartments and thus to participate in receptor cargo collection during the formation of transport intermediates. Rab proteins also interact with other effectors to mediate accurate docking and the fusion of transport vesicles with their target membranes (Zerial and McBride, 2001).

Rab11 plays an essential part in the transport of membrane proteins through the recycling compartment of the early endosomal pathway. Its activity seems to be finely regulated by numerous Rab11-interacting proteins, such as Rab11-FIPs, Evi5, or Myosin Vb (Meyers and Prekeris, 2002; Lapierre and Goldenring, 2005; Westlake *et al*., 2007). Several convergent arguments suggest that different and even mutually exclusive Rab11-interacting complexes, with distinct functions, coexist within cells (Meyers and Prekeris, 2002). Thus, the RCP–Rab11 complex regulates recycling of the transferrin receptor (TfR), but not that of epidermal growth factor receptor (EGFR) (Peden *et al*., 2004). In contrast, silencing of another Rab11-interacting protein, Rip11, does not seem to affect TfR recycling or stability (Peden *et al*., 2004), suggesting that Rab11–Rip11 forms part of another Rab11 complex. The concept that the recycling of plasma membrane receptors is specifically regulated by different Rab11-interacting proteins has been mainly tested with a limited

This article was published online ahead of print in *MBC in Press* (http://www.molbiolcell.org/cgi/doi/10.1091/mbc.E06–09–0779) on May 30, 2007.

[D] The online version of this article contains supplemental material at *MBC Online* (http://www.molbiolcell.org).

Address correspondence to: Jean Salamero (jean.salamero@curie.fr) or Daniel Hanau (daniel.hanau@efs-alsace.fr).

Abbreviations used: BG, Birbeck granule; ERC, endosomal recycling compartment; LC, Langerhans cell; siRNA, small interfering RNA; TfR, transferrin receptor.

number of classical cargos, such as TfR or EGFR. Moreover, this has rarely been validated in differentiated cellular systems (Nedvetsky *et al*., 2007).

Rab11 has been shown to regulate not only the recycling of plasma membrane receptors (Ullrich *et al*., 1996) but also transport from early endosomes to *trans*-Golgi network (TGN) membranes (Wilcke *et al*., 2000), exocytosis from or via the recycling endosomes (Kessler *et al*., 2000; Lock and Stow, 2005), cholesterol homeostasis (Holtta-Vuori *et al*., 2002), and recruitment of membranes to the cell periphery (Cox *et al*., 2000; Savina *et al*., 2002, 2005). These different transport pathways may all be based on similar Rab11-mediated mechanisms, but they depend most almost certainly on different Rab11-interacting partners and on cell type specificities. Moreover, Rab11 is associated not only with TGN membranes and recycling endosomes but also, in differentiated cells, with exocytic vesicles or tubules, which may be related to the recycling pathway (Calhoun *et al*., 1998; Savina *et al*., 2005; Ward *et al*., 2005).

Epidermal Langerhans cells (LCs) represent a subset of dendritic cells containing characteristic organelles, the Birbeck granules (BGs) (Birbeck *et al*., 1961). These distinctive rod-shaped compartments display a remarkable association with Rab11. LCs uniquely express a C-type lectin called Langerin (Valladeau *et al*., 1999), which is necessary for the formation of BGs (Valladeau *et al*., 2000). This protein is expressed on the plasma membrane and constitutively internalized into BGs, the internal membranes where it accumulates (Valladeau *et al*., 2000; Mc Dermott *et al*., 2002), before returning to the plasma membrane (Mc Dermott *et al*., 2002). Thus, the major intracellular pool of Langerin is the Rab11$^+$ BGs, which correspond to subdomains of the endosomal recycling compartment (ERC) of LCs (Mc Dermott *et al*., 2002). We have developed transfected cell lines expressing Langerin (M10-22E, HeLa-Langerin) as a cellular model of BG biogenesis. In these cells, Langerin colocalizes with TfR and Rab11, and it recycles as in LCs (McDermott *et al*., 2004). In this study, we investigated the role of Rab11A and different Rab11-interacting proteins in the traffic and steady-state distribution of Langerin and the membrane organization and biogenesis of BGs.

## MATERIALS AND METHODS

### *Cell Lines*

The Langerin-transfected cell line M10-22E was maintained in culture as described previously (McDermott *et al*., 2004). Langerin cDNA was inserted into the pSVZeo expression vector (Invitrogen, Carlsbad, CA), and the resulting plasmid was used to transfect HeLa cells, by using FuGENE transfection reagent (Roche Diagnostics, Basel, Switzerland). Stable clones were selected on 750 $\mu$g/ml Zeocin (Invitrogen), and they were screened for Langerin and BG expression.

### *Antibodies and Reagents*

The mouse monoclonal antibodies (mAbs) used were as follows: DCGM4 (IgG1, anti-Langerin/CD207; Immunotech, Marseille, France), DF 1513 (IgG1, anti-CD71/TfR; Sigma-Aldrich, St. Louis, MO), H68.4 (anti-CD71/TfR; kindly provided by I. Trowbridge, The Salk Institute, San Diego, CA), 6C4 (anti-lysobisphosphatidic acid [LBPA]; Kobayashi *et al*., 1998; kindly provided by J. Gruenberg, University of Geneva, Switzerland), anti-calnexin (BD Biosciences, Le Pont de Claix, France), anti-Rab5 (BD Biosciences), and TUB 2.1 (anti-$\beta$-tubulin; Sigma-Aldrich). A goat anti-EEA1 mAb (N-19) was obtained from Santa Cruz Biotechnology (Santa Cruz, CA), and a chicken anti-RCP mAb was from GenWay Biotech (San Diego, CA). Polyclonal rabbit antibodies (Abs) were raised against 1) full-length recombinant Rab11A produced in *Escherichia coli* and affinity purified as described previously (Martinez *et al*., 1994; Wilcke *et al*., 2000); and 2) the peptide sequence Tyr-Met-Thr-Val-Glu-Lys-Glu-Ala-ProAsp-Ala-His-Phe-Thr-Val-Asp-Lys-Gln, corresponding to part of the cytoplasmic tail of Langerin (Neosystems, Strasbourg, France and Eurogentec, Herstal, Belgium). Rabbit polyclonal IgG against Rab6 or Rab4 and rabbit polyclonal immunoglobulin (Ig)G against CD40 were purchased from Santa Cruz Biotechnology. An affinity-purified rabbit antibody against Rip11 was kindly provided by R. Prekeris (University of Colorado, Aurora, CO). Horseradish peroxidase (HRP)-conjugated donkey anti-rabbit, anti-chicken, or anti-mouse IgG (H+L) were obtained from Jackson ImmunoResearch Laboratories (West Grove, PA), whereas the enhanced chemiluminescence substrate for HRP detection was provided by Pierce Chemical (Rockford, IL). Cy3- or Cy5-conjugated donkey anti-mouse, anti-rabbit, or anti-goat IgG (H+L) (Jackson ImmunoResearch Laboratories) and A488-conjugated donkey anti-mouse or anti-rabbit IgG (Invitrogen) were used for indirect immunofluorescence staining for confocal microscopy. DCGM4 was labeled with 6-nm gold particles as previously described (Mc Dermott *et al*., 2002). HRP and invertase (grade VII) from baker's yeast were provided by Sigma-Aldrich, and HRP-conjugated mouse transferrin (Tf) was purchased from Pierce Chemical. Invertase was directly coupled to Cy3 with a Cy3-link kit (GE Healthcare, Little Chalfont, Buckinghamshire, United Kingdom) according to the manufacturer's instructions. DMEM depleted of methionine and cysteine was obtained from Invitrogen, $^{35}$S Translabel was from MP Biomedicals (Irvine, CA), and protein G-Sepharose was from GE Healthcare.

### *Recombinant Rab4 and Rab11A Adenoviruses*

PEGFP-Rab11AWT, -Q70L, and -S25N were generously provided by G. Langsley (Institut Pasteur, Paris, France). Cells were transfected by the calcium phosphate precipitation method (Jordan *et al*., 1996). Recombinant adenovirus vectors encoding the various enhanced green fluorescent protein (EGFP)–Rab4 (S22N, Q67L) and EGFP–Rab11A (S25N, Q70L) mutated fusion proteins were obtained by subcloning into pTG13387 (provided by Transgène SA, Strasbourg, France). The complete recombinant adenovirus genome was reconstituted as described by Chartier *et al*. (1996), and adenoviruses were amplified in the complementary LCA4 cell line (Transgène SA) as described by Imler *et al*. (1996). Cells were infected by incubation with various amounts of virus for 18–20 h in culture medium containing only 2% fetal calf serum (FCS). When indicated, 50 $\mu$M chloroquine (Sigma-Aldrich) was added for the last 12 h of infection.

### *Immunofluorescence, Confocal Microscopy, and Image Analysis*

Immunofluorescence images were acquired by confocal microscopy of fixed, permeabilized cells as described previously (Mc Dermott *et al*., 2002), using a Leica SP2-AOBS confocal microscope (Leica Microsystems, Heidelberg, Germany). For quantitative purposes, the cells were also examined under an upright motorized epifluorescent microscope (Leica DMRA2) equipped with a 100× PL APO HCX 1.4 numerical aperture objective and an interlined charge-coupled device camera (CoolSnap HQ; Roper, Scientific, Trenton, NJ). The system was controlled with MetaMorph software (Molecular Devices, Sunnyvale, CA). Stacks of 25–30 images, taken with a 0.2-$\mu$m plane to plane distance in each fluorescence channel of interest, were submitted to three-dimensional (3D) projection, and the resulting composite images were used for quantitative analysis of the fluorescence intensity/cell, using MetaMorph software. Some of these stacks were deconvolved with the MetaMorph Fast Iterative Constrained PSF-based algorithm (Agard *et al*., 1989), to improve the resolution of the fluorescent signals in the multifluorescent images. More precisely, 3D stacks of images were acquired for the green fluorescent protein (GFP) and Cy3 or Cy5 fluorescent signals, by using a fixed exposure time for each channel (100 ms for GFP and 200 ms for Cy3 or Cy5). Special care was taken to record nonsaturating images with a high dynamics of the pixels in the GFP channel (S/N always >700 Gy levels and pixel size of at least 12 bits). The resulting 3D projections of the staining in each cell were then produced and quantified using MetaMorph software, by selecting individual cells as a region of interest to be measured in both channels, taking into account the background signals and the total size of the cells.

### *Internalization of Tf and Invertase*

M10-22E cells were incubated with Cy3-invertase or Cy3-Tf in 10 $\mu$g/ml RPMI 1640 medium for 60 min at 37°C. The cells were then either fixed directly or permeabilized and processed for multiple labeling, as described previously (Mc Dermott *et al*., 2002).

### *Immunoelectron Microscopy*

Langerin$^+$ HeLa cells were fixed at 37°C (Mc Dermott *et al*., 2002), and ultrathin sections were examined under a Philips CM 120 BioTwin electron microscope (120 kV) (Philips, Eindhove, The Netherlands).

M10-22E cells were either infected for 18–20 h with recombinant adenoviruses or microinjected with small interfering RNA (siRNA) for 48 h. During the last 30 min of infection or RNA interference, 10 mg/ml HRP, and/or a gold-labeled anti-Langerin mAb (final dilution 1:100) were added to the incubation mixture. HRP was detected by processing the cells as described previously (Mc Dermott *et al*., 2002). In the absence of HRP, the cells were fixed with glutaraldehyde and sucrose.

### *RNA Interference*

The siRNA sequences designed to target human *RAB11A* were synthesized at QIAGEN (Courtaboeuf, France). These sequences, against two different regions of the Rab11A gene, were siRNA-Rab11A1: sense (5′-GAGUGAUCUACGUCAUCUCd(TT)-3′) and siRNA-Rab11A2: sense (5′-GAGCGAUAUCGAGCUAUAAd(TT)-3′). siRNA duplexes (QIAGEN) were prepared according to the manufacturer's instructions. The siRNA sequence against Rab4A (sense 5′-GCCAGAACAUUGUGAUCAUd(TT)-3′) was kindly provided by M. Cormont (Faculté de Médecine de Nice, Nice, France). The siRNAs against Rab6A/A′ (Del Nery *et al*., 2006) and against Rab5A were published previously (Huang *et al*., 2004), whereas the siRNAs against RCP and Rip11 were described by Peden *et al*. (2004). Cells were transfected with the siRNAs, by using Lipofectamine 2000 (Invitrogen) according to the manufacturer's instructions. Mock-transfected cells were treated similarly, except that the siRNA was replaced by $H_2O$. After 72 h, the efficiency of siRNA silencing was assessed by immunofluorescence assays with polyclonal rabbit anti-Rab11 antibodies and by immunoblotting. Alternatively, the siRNAs were microinjected into M10-22E cells grown on coverslips, by using a manual microinjector (TransferMan NK2; Eppendorf, Hamburg, Germany). The relevant 5 $\mu$M siRNA was diluted in microinjection buffer (5 mM sodium phosphate buffer, pH 7.2, and 100 mM KCl) containing 40 kDa of neutral dextran-Texas Red (Invitrogen). Microinjections were carried out in a delimited area of the cell, and they were detected on the basis of dextran-Texas Red staining. The efficiency of siRNA silencing was assessed 48 h after microinjection, by immunofluorescence assays with polyclonal rabbit anti-Rab11 antibodies. When indicated, 50 $\mu$M chloroquine (Sigma-Aldrich) was added for the last 12 h of siRNA treatment.

### *Western Blotting, Metabolic Labeling, and Immunoprecipitation*

In immunoblotting assays, the cells were washed twice with phosphate-buffered saline (PBS) and incubated for 20 min at 4°C in lysis buffer (150 mM NaCl, 20 mM imidazole, pH 7.2, 0.5% Triton, and 10 mM $MgCl_2$) supplemented with protease inhibitor cocktail (Sigma-Aldrich). Protein concentrations were determined with the Bio-Rad Protein Assay (Bio-Rad, Munich, Germany), and cell extracts were analyzed by SDS-polyacrylamide gel electrophoresis (PAGE) on 12% polyacrylamide gels. Pulse-chase and immunoprecipitation experiments were carried out essentially as described previously (Angenieux *et al*., 2005). The cells were pulse labeled with [$^{35}$S]methionine and cysteine (Translabel) for 30 min at 150 $\mu$Ci per $2 \times 10^6$ cells in a volume of 1 ml, and then they were chased for various times in a suspension containing $4 \times 10^6$ cells/ml in RPMI 1640 medium supplemented with 10% FCS. When specified, 50 $\mu$M chloroquine (Sigma-Aldrich) or 20 $\mu$M MG132 (Calbiochem, San Diego, CA) was added to the chase medium. At the indicated times, the cells were chilled in ice-cold PBS, washed, and solubilized in 1 ml of ice-cold lysis buffer. After preclearing twice with 90 $\mu$l of protein G-Sepharose (GE Healthcare), each time for 2 h at 4°C, the lysates were incubated overnight with protein G-Sepharose and 5–10 $\mu$g of the relevant Abs at 4°C. The lysates were then thoroughly washed, and the immunoprecipitates were separated by SDS-PAGE on 12% polyacrylamide gels under reducing conditions. The gels were developed with PhosphorImager (GE Healthcare). Quantitative analysis of Western blots was performed with ImageJ software (National Institutes of Health, Bethesda, MD).

## RESULTS

### *The Cellular Distributions of Langerin and Tfr Are Modified by Overexpression of a Constitutively Active Rab11A Mutant*

To investigate the role of Rab11 in control of the cellular distribution of Langerin, M10-22E cells were transduced with recombinant adenoviruses encoding a constitutively active GFP–Rab chimeric protein (GFP–Rab11AQ70L). This produced almost uniform levels of expression of the mutated Rab11A. Compared with noninfected cells (Figure 1A), where Rab11A and Langerin staining were mainly coincident in the pericentriolar area (Figure 1A, inset), overexpression of Rab11A WT (data not shown) or low (8 $\mu$l of stock solution of adenoviruses; Figure 1B) or high (20 $\mu$l of stock solution of adenoviruses; Figure 1C) expression of Rab 11AQ70L led to partial redistribution of Langerin to the cell periphery. In most Rab11AQ70L-infected cells, cellular protrusions were immunolabeled with the anti-Langerin mAb DCGM4, whereas the distribution of chimeric GFP–Rab11A molecules somewhat overlapped with that of Langerin (see overlays and insets in Figure 1, B and C, where the overall green staining has been reduced to better visualize the yellow-orange overlaps).

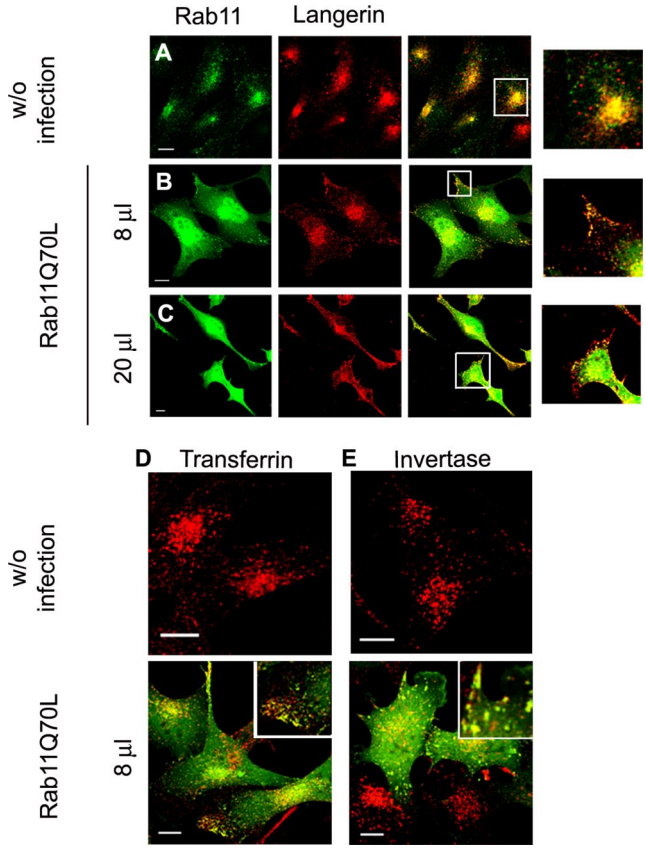


**Figure 1.** Effects of Rab11AQ70L overexpression on Langerin distribution and transferrin and invertase internalization in M10-22E cells. As a control, untransduced M10-22E cells (A) were labeled with anti-Rab11 serum revealed with donkey anti-rabbit A488 and with the anti-Langerin mAb DCGM4 revealed with donkey anti-mouse Cy3. Cell transductions were carried out as described in *Materials and Methods* by using low (8 $\mu$l of stock solution) (B) or high (20 $\mu$l of stock solution) (C) concentrations of recombinant adenoviruses encoding the constitutively active chimeric protein GFP–Rab11AQ70L. Eighteen to 20 h after transduction, the cells were labeled with DCGM4 (B and C) revealed with donkey anti-mouse Cy3. Untransduced cells (top) and GFP-Rab11AQ70L-transduced cells (bottom) were incubated with either Cy3-transferrin (D) or Cy3-invertase (E) for 1 h at 37°C before fixation. All image acquisition parameters were identical for B and C. Insets at higher magnification are included to improve the visualization of structural details in the merged images (A–C and E). To allow a better appreciation of the occurrence of colocalization, the fluorescence signal corresponding to the GFP channel was manually reduced in the zoomed images of B and C. Bars, 10 $\mu$m.

Previous studies have shown that changes in the intracellular distribution of recycling proteins induced by Rab11A mutant proteins arise from changes in the kinetics of the traffic of these cargo molecules (Ullrich *et al*., 1996; Ren *et al*., 1998; Wilcke *et al*., 2000). Hence, the changes in Langerin distribution induced by the overproduction of Rab11A mutant proteins might also result from changes in Langerin traffic. Because this lectin has been shown to bind in vitro to mammalian high-mannose oligosaccharides and even more strongly to the polysaccharide moieties of yeast invertase (Stambach and Taylor, 2003), through its carbohydrate recognition domain, we used fluorescently labeled invertase

(Cy3-invertase) to follow the fate of internalized invertase–Langerin complexes.

M10 and M10-22E (Langerin$^+$) cells were incubated for 1 h at 37°C with Cy3-invertase or Cy3-Tf. Invertase was taken up exclusively by M10-22E cells through binding to Langerin (data not shown). After endocytosis, most of the Cy3-invertase was found in Langerin$^+$ compartments (Supplemental Figure S1A). Immunolabeling revealed strong colocalization of the internalized invertase with Rab11 and TfR in the pericentriolar region (Supplemental Figure S1, B and C), whereas no coimmunostaining was detected in the late endosomes/lysosomes labeled with the mAb 6C4 (Kobayashi *et al.*, 1998) (Supplemental Figure S1D).

We then looked at the effects of the constitutively active Rab11A mutant on the intracellular distribution of invertase and Tf. Overproduction of GFP–Rab11AQ70L led to the redistribution of intracellular invertase and Tf to the cell periphery (compare the invertase and Tf signals in Figure 1, D and E, top and bottom, respectively). In both cases, the peripheral labeled structures also corresponded to sites of GFP–Rab11AQ70L accumulation (Figure 1, D and E, insets, bottom).

### *An Active Rab11A Protein Is Needed for Normal Distribution and Expression of Langerin*

The similar behavior of TfR and Langerin after perturbation of the membrane dynamics by Rab11A mutants was confirmed by an almost complete coincidence of their distribution in cells overexpressing the GFP chimera of the dominant-negative mutant Rab11AS25N (Figure 2A). In M10-22E cells, both proteins were redistributed into a tubular network of endosomal membranes induced by overexpression of Rab11AS25N, a phenotype often observed in mammalian cells (Wilcke *et al.*, 2000; Holtta-Vuori *et al.*, 2002) (Figure 2A, overlay and inset). More precisely, this was true only when low doses of GFP-Rab11AS25N adenoviruses were used (Figure 2B, 2 $\mu$l of stock solution), whereas higher expression of Rab11AS25N (10 $\mu$l of stock solution) led to a decrease in Langerin in the M10-22E cell line, as seen on confocal micrographs (Figure 2C) and shown by quantification of fluorescence signals (Figure 2D). On the basis of these quantitative analyses of the fluorescence intensity per cell, we could estimate that a dose of 10 $\mu$l of GFP–Rab11AS25N induced a sixfold increase in expression of the Rab11A mutant compared with a dose of 2 $\mu$l of GFP–Rab11AS25N. This was sufficient to promote a statistically significant (~1.8-fold) decrease in the Langerin content of the cells, as assessed by DCGM4 immunostaining. Compared with Langerin immunostaining in mock-transfected cells, the reduction reached a factor of 2.1.

Remarkably, although low levels of dominant-negative Rab11A led to the expected changes in the distribution of internalized Tf (Figure 2E, left) (Wilcke *et al.*, 2000; Holtta-Vuori *et al.*, 2002), it abolished the internalization of invertase in M10-22E cells (compare Figure 2E, right, with the staining of internalized invertase in Supplemental Figure S1). The internalization of Tf and its accumulation in tubular structures indicates that the effect of Rab11AS25N on Langerin traffic was specific, rather than a general effect on the endocytic recycling pathway.

As a control for the specificity of Rab11A, we also analyzed the distribution of Langerin in cells infected with equivalent mutants of Rab4, a Rab protein involved in the fast recycling of TfR (van der Sluijs *et al.*, 1992; Mohrmann *et al.*, 2002). The distribution of Langerin was not affected by overproduction of the dominant-negative mutant GFP–Rab4S22N, whereas cells overproducing the constitutively active mutant GFP–Rab4Q67L accumulated Langerin in many enlarged Rab4$^+$ structures (Supplemental Figure S2B). These enlarged structures occurred at the ultrastructural level as small "multivesicular" endosomes connected or

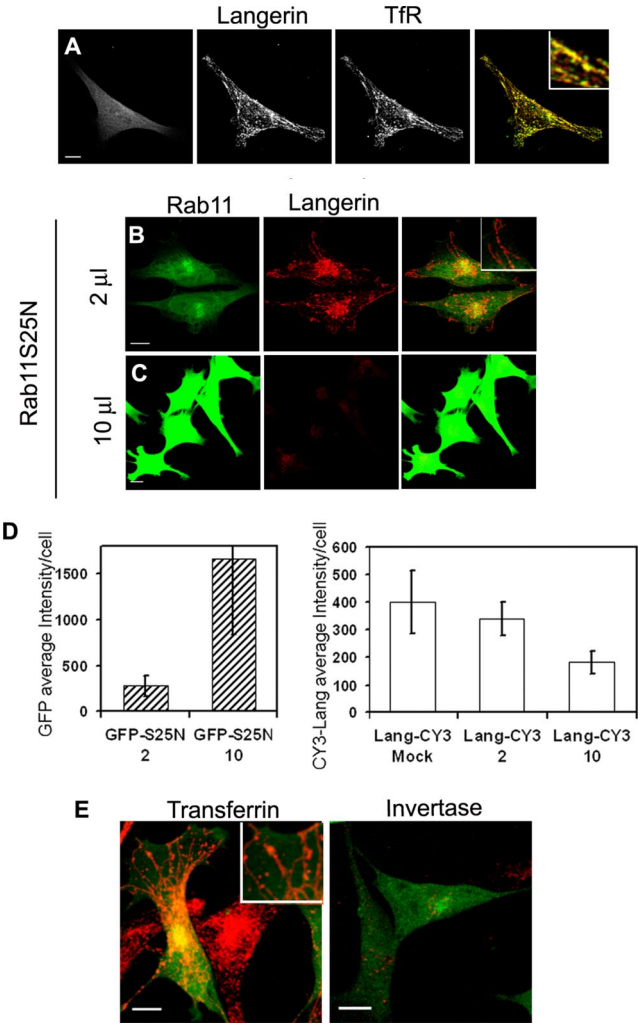


**Figure 2.** Effects of Rab11AS25N overexpression on Langerin levels and distribution and transferrin and invertase internalization in M10-22E cells. Cells infected with GFP–Rab11AS25N (A, left) were labeled with an antiserum against the cytoplasmic domain of Langerin revealed with anti-rabbit Cy3 (A, middle) and with an anti-TfR mAb revealed with anti-mouse Cy5 (A, right). The overlay image in A corresponds to the merging of Langerin and TfR staining and shows that the distributions of the two molecules are strongly correlated. Cells transduced with two different doses (2 $\mu$l of stock solution (B) or 10 $\mu$l (C)) of recombinant adenoviruses encoding the dominant-negative mutant GFP–Rab11AS25N were labeled with the anti-Langerin mAb DCGM4 (B and C) revealed with donkey anti-mouse Cy3. Bars, 10 $\mu$m. All images were acquired with an SP2 AOBS confocal microscope. The fluorescence intensities of GFP-Rab11AS25N and Langerin (D) were quantified as described in *Materials and Methods* by using stacks of images acquired with a wide-field microscope. Values are means ± SD of the average intensity per cell with n = 19, 29, and 23 cells for the mock, 2- and 10-$\mu$l experimental conditions, respectively. Cells infected with a low dose (2 $\mu$l) of GFP–Rab11AS25N were incubated with 10 $\mu$g of Cy3-transferrin (E, left) or Cy3-invertase (E, right) for 1 h at 37°C. Higher magnification insets are included to improve the visualization of structural details in the merged images (A, B, and E). Bars, 10 $\mu$m.

close to BGs (Supplemental Figure S3, B–D). We also looked at the effects of Rab4 mutant proteins on the internalization and distribution of invertase. Rab4S22N had no effect on the distribution of invertase, whereas overproduction of Rab4Q67L led to its accumulation in enlarged Rab4$^+$ structures (Supplemental Figure S2F). Similarly, internalized Tf was found in the enlarged Rab4$^+$ compartments of cells overproducing Rab4Q67L (Supplemental Figure S2D). Despite these significant effects of Rab4Q67L on the distributions of Langerin, internalized invertase, and Tf, none of the Rab4 mutant proteins tested abolished invertase internalization (Supplemental Figure S2), in marked contrast to the effect of the dominant negative form of Rab11A.

Altogether, the aforementioned results indicate that dominant-negative Rab11A mutant proteins strongly affect the traffic of Langerin–invertase complexes and that strong expression of such a mutant leads to a loss of Langerin expression.

### *Rab11AS25N Induces a Missorting of Langerin*

We next investigated why the Langerin content of cells depended on the level of GFP–Rab11AS25N mutant. Figure 3B (left) illustrates the dose-dependent effect of Rab11AS25N on the expression of Langerin in M10-22E cells. Overexpression of Rab11AS25N led to a marked decrease in Langerin expression. Interestingly, this mainly concerned the high-molecular-weight forms of Langerin, which correspond to modifications of the carbohydrate moieties of the protein (Valladeau *et al*., 1999; Stambach and Taylor, 2003). We also observed a slight decrease in TfR expression at high doses of the mutant, although this was not reproducible in three independent experiments. Quantitative analysis of the expression of GFP–Rab11AS25N by immunoblotting with an anti-GFP antibody confirmed that the high dose (10 $\mu$l) of adenoviruses induced a 4–5 times increase in Rab11AS25N expression, compared with the low dose (2 $\mu$l). Immunoblotting with an anti-Rab11 antibody (Figure 3A) further indicated that the low dose of adenoviruses already induced a five- to sixfold increase in the expression of the GFP–Rab11A chimera compared with endogenous Rab11. The effect of Rab11AS25N on Langerin expression was overcome when chloroquine was added to the cells during the last 12 h of infection (Figure 3B, right). This recovery mainly concerned the high-molecular-weight forms of Langerin. In contrast, no significant change in levels of TfR expression was observed in cells treated or not with chloroquine during infection with various doses of Rab11AS25N. Some apparent differences on the TfR immunoblots were due to experimental variability and not comparable with the important variations in Langerin expression. The chloroquine treatment also restored the immunofluorescent Langerin signal in cells overexpressing Rab11AS25N (Figure 3C) but notably not the capacity of these cells to internalize invertase (Figure 3D). Together, these results indicate that the presence of an active Rab11A protein allows the biogenesis of a functional ERC, where Langerin can be stored. In the absence of active Rab11A, Langerin is diverted to the late endosomal network for degradation, whereas TfR recycling is still possible.

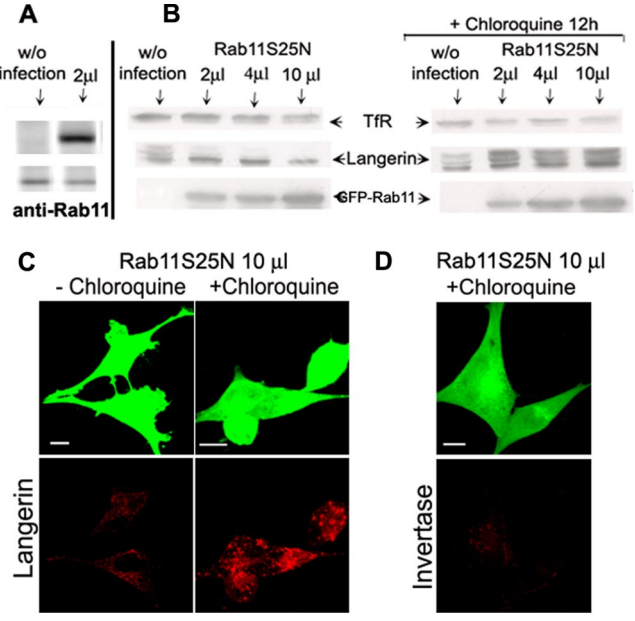


**Figure 3.** Effects of Rab11AS25N overexpression on Langerin levels in M10-22E cells. Immunoblotting was used to compare the levels of TfR, Langerin, and GFP–Rab11A in uninfected cells and cells infected with increasing amounts (2, 4, or 10 $\mu$l) of Rab11AS25N adenoviruses, in the presence (B, right) or absence (B, left) of 50 $\mu$M chloroquine, as described in *Materials and Methods*. Proteins were separated by SDS-PAGE in 12% acrylamide gels and blotted onto membranes, with equivalent amounts of protein being loaded in each lane. The positions of TfR, Langerin, and GFP–Rab11A are indicated by arrows. Blots are representative of three independent experiments with individual blots being probed for all three proteins. As a control for endogenous Rab11 versus GFP–Rab11AS25N expression, both proteins were probed with anti-Rab11 antibodies in uninfected cells (without infection) and cells infected with 2 $\mu$l of GFP–Rab11AS25N adenoviruses (A). M10-22E cells infected with 10 $\mu$l of Rab11AS25N were incubated with (C, right, and D) or without (C, left) 50 $\mu$M chloroquine, as described in *Materials and Methods*. The cells were then immunolabeled with the anti-Langerin mAb DCGM4 (C) or incubated with Cy3-invertase for 1 h at 37°C before fixation (D).

### *Rab11A Activity Regulates Birbeck Granule Biogenesis*

Langerin induces the formation of BGs in areas where it accumulates (Valladeau *et al*., 2000; McDermott *et al*., 2004), but the cellular distribution and traffic of Langerin are controlled by Rab11A (Figures 1 and 2). We therefore investigated the fate and distribution of BGs in M10-22E cells expressing active or dominant-negative forms of Rab11A.

In cells expressing GFP–Rab11AQ70L, electron microscopy revealed the presence of several open-ended, coated BG-like structures appended to the cell surface (Figure 4A), which are not observed in nontransduced cells (McDermott *et al*., 2004), along with many cytosolic BGs displaying classical morphological features, mostly redistributed close to the plasma membrane (Figure 4, B and C). These BGs were continuous with vacuolar (Figure 4B) and tubular membrane structures (Figure 4C) (for comparison, see Supplemental Figure S3A).

In contrast, extensive vacuolar (Figure 4D) and tubular (Figure 4, D and E) endosomal networks (highlighted here by the presence of a few gold-labeled anti-Langerin mAbs in the higher magnification of Figure 4E) were found in M10-22E cells expressing relatively low levels of Rab11AS25N, which weakly affect levels of Langerin (see experimental conditions in Figure 2, B and D). The relative proportions of these networks depended on the cell. BGs were, however, exceedingly rare, small, and incomplete in all the cells. Occasionally, we observed small tubular structures resembling BGs, characterized by very short, thin, central "striations," either connected to the tubular network or apparently isolated in the cytosol (Figure 4F). These results suggest that Rab11A is involved in the biogenesis of BGs.

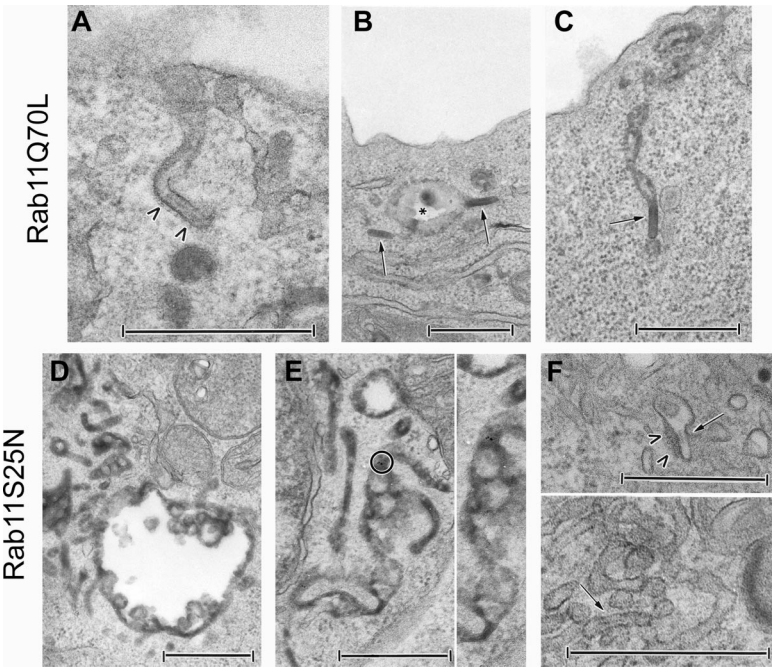


**Figure 4.** Effects of Rab11A recombinant adenoviruses on the distribution and presence of Birbeck granules in M10-22E cells. M10-22E cells were transduced with recombinant adenoviruses encoding GFP–Rab11AQ70L (20 $\mu$l [?] of stock solution) (A–C) or GFP–Rab11AS25N (2 $\mu$l of stock solution) (D–F), in the presence of 10 mg/ml HRP and/or a gold-labeled anti-Langerin mAb during the last 30 min of infection. An open-ended "BG-like structure" appended to the cell surface and coated over its entire length (arrowheads) is shown in A. Cytosolic BGs (arrows) are essentially located at the cell periphery, close to the plasma membrane. They are either isolated (B) or continuous with vacuolar endosomal structures (star) (B) and tubular membrane structures (C). As shown in D and E, tubular and vacuolar HRP$^+$ networks occur in M10-22E cells expressing Rab11AS25N, with variable proportions of each type of network between cells. Thus, the vacuolar component is readily seen in D, whereas the tubular component predominates in E. These networks are linked to the early endosomal pathway, as shown by the occasional presence of gold-labeled anti-Langerin mAbs (a gold-labeled area in E is circled and enlarged on the right-hand side). In contrast, BGs are absent from these tubular networks. Only very occasionally (F), small tubular structures resembling BGs (arrow) with a very short, thin, central striation and a surrounding coat (arrowheads) can be seen, either apparently isolated in the cytosol or connected to the tubular network. Bars, 0.5 $\mu$m.

### *Rab11A Is Essential for Langerin Stability*

RNA interference was used to knock down Rab11A levels and thereby confirm the involvement of Rab11A in the maintenance and biogenesis of BGs. Two complementary approaches were used, with two different cell types, to overcome potential problems associated with cell type-specific effects and differences in RNA interference efficiency.

We used a stably transformed HeLa cell line producing Langerin for biochemical analyses at the cellular level. The production and distribution of Langerin were investigated by immunolabeling with DCGM4 (Figure 5A), whereas the presence and morphology of BGs were checked by electron microscopy (Figure 5B). First, the efficiency of the RNA interference induced by the oligonucleotides Rab11A2 (data not shown) and Rab11A1 was demonstrated by comparing the Rab11 labeling in treated cells (Figure 5D, left) and mock-treated cells (Figure 5C, left). Cells producing no or small amounts of Rab11 clearly showed weaker DCGM4 (anti-Langerin) labeling (Figure 5D, middle) than control cells (Figure 5C, middle). Consistent with the immunofluorescence data, Western blotting showed that RNA interference with the Rab11A1 oligonucleotides resulted in almost complete loss of the Rab11 signal (Figure 5E). Rab11A knockdown decreased Langerin levels but, to our surprise, it had no significant effect on TfR expression (Figure 5E). The decrease in Langerin levels was specifically correlated with a loss of Rab11A expression, because siRNA against Rab4A, Rab5A, or Rab6A/A′ (Figure 5E) strongly reduced the respective Rab signal, without significantly modifying the Langerin signal. Conversely, because the molecular weight pattern of Langerin in transfected HeLa cells was not identical to that in M10-22E cells (Figure 3B), it was difficult to correlate the effects produced by overexpression of Rab 11AS25N mutants and siRNA knockdown of Rab11A. We then carried out pulse-chase experiments, in the presence or absence of chloroquine, to determine whether the loss of Langerin in HeLa cells treated with Rab11A siRNA was due to defective de novo Langerin synthesis or its degradation in late endosomal compartments, as suggested by the experiments with the Rab11AS25N mutant in M10-22E cells (Figure 3B). After a 30-min pulse (t0), newly synthesized Langerin was found in both siRNA- and mock-treated cells (Figure 5F), which excluded the possibility of a significant effect of Rab11A siRNA on transcriptional or translational processes. Mock- and siRNA-treated cells were treated or not for 12 h with chloroquine before each time point, including t0. Under these conditions, the newly synthesized Langerin occurred both as an immature form (Figure 5F, lower band), and already in more mature glycosylated forms (top bands). At early time points of the chase (1, 3, and 6 h), no significant differences between chloroquine-treated and untreated cells could be detected (data not shown). After 12 h of chase, Langerin occurred as a single protein band of higher molecular weight, the intensity of which was weaker after treating the cells with Rab11A siRNA (Figure 5F), but it was restored by chloroquine treatment. We also tested inhibitors of other degradative pathways such as MG132, a specific inhibitor of proteasome activity, but we found no rescue of Langerin in cells treated with Rab11A siRNA (data not shown). Thus, Rab11A knockdown in Langerin$^+$ HeLa cells did not impair de novo Langerin synthesis, but it did affect Langerin turnover. We conclude that Rab11A siRNA specifically decreases the stability of Langerin by inducing its missorting to the endosomal–lysosomal degradative pathway.

### *Rab11A Is Essential for Birbeck Granule Biogenesis*

The observation that Langerin expression could be rescued by chloroquine treatment in cells knocked down for Rab11A or overexpressing Rab11S25N led us to investigate the relative importance of Langerin and Rab11A in BG formation. This ultrastructural analysis was performed in the M10-22E cell line, which has been shown to be homogeneous in terms of Langerin production and BG density. As shown in Figure 6A, after simultaneous microinjection of Rab11A1 siRNA, Rab11 was no longer detectable (Figure 6A, middle). Rab11A knockdown also decreased Langerin expression (Figure 6A, right), as in siRNA-treated Langerin$^+$ HeLa cells

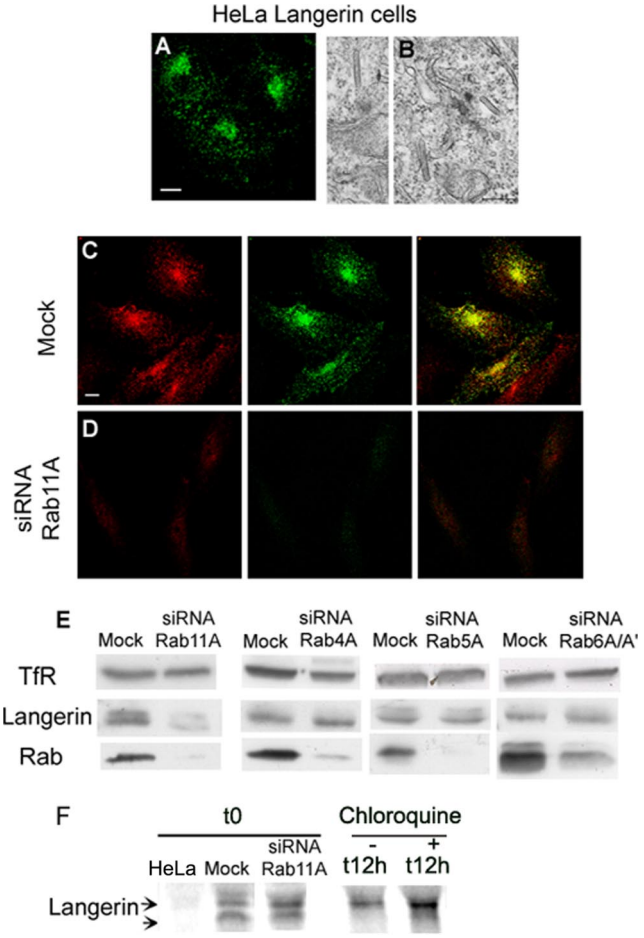


**Figure 5.** Effects of Rab11A knockdown on Langerin levels in Langerin$^+$ HeLa cells. Transfected HeLa cells expressing Langerin were analyzed by immunofluorescence after staining with the anti-Langerin mAb DCGM4 (A), and the presence of BGs was checked by electron microscopy (B). Langerin$^+$ HeLa cells were either mock treated (C) or treated with Rab11A1 siRNA (D) for 72 h, before labeling with either an anti-Rab11 serum (red) or the anti-Langerin mAb (green). Note the high efficiency of Rab11A knockdown in Langerin$^+$ HeLa cells (compare C and D, for which the acquisition parameters were identical). The distributions of the two molecules are strongly correlated in untreated cells (C), whereas the extinction of Langerin parallels the knockdown of Rab11A (D). These images are representative of five independent experiments. Bars, 10 $\mu$m. Levels of TfR, Langerin, Rab11, Rab4, Rab5a, and Rab6 in mock-treated cells (mock) or cells treated with siRNA against Rab11A, Rab4A, Rab5A, or Rab6A/A' were assayed by immunoblotting (E). The data shown are representative of five independent experiments for Rab11A siRNA (see Figure 7B for a quantitative analysis) and two independent experiments for the other siRNAs. Proteins were separated by SDS-PAGE in 12% acrylamide gels and blotted onto membranes. Equivalent amounts of total protein were loaded in each lane, and all proteins were tested on the same blots. Metabolic labeling of Langerin$^+$ HeLa cells (F) treated with Rab11A siRNA was followed by immunoprecipitation of Langerin. Pulse-labeled Langerin$^+$ HeLa cells transfected with Rab11A siRNA were also treated (+) or not (−) for various chase times with 50 $\mu$M chloroquine. Time 0 (t0) corresponds to the Langerin immunoprecipitate in cells transfected with Rab11A1 siRNA or not (mock) and metabolically labeled for 30 min. Langerin was also immunoprecipitated from normal HeLa cells under identical conditions and time 0 of a pulse-chase experiment is presented here. In samples treated with chloroquine for the previous 12 h, the Langerin signal is found in a lower band corresponding to the newly synthesized immature form of the molecule. After only 30 min of chase, higher bands corresponding to more mature forms of the glycoprotein already occur

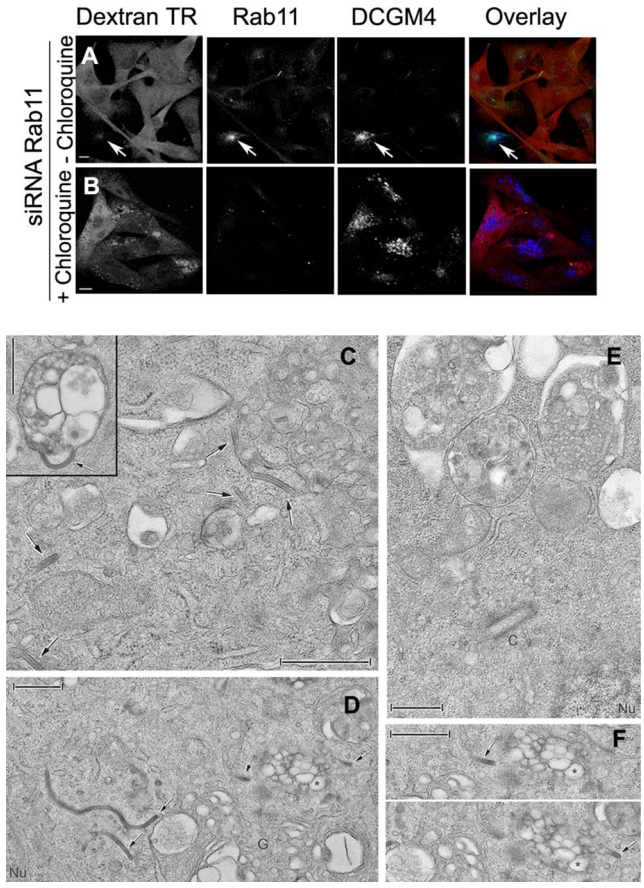


**Figure 6.** Birbeck granule formation requires the presence of both Langerin and Rab11A. M10-22E cells, comicroinjected with siRNA against Rab11A and Texas Red-dextran (A and B, left [red]), were incubated with (B) or without (A) 50 $\mu$M chloroquine, as described in *Materials and Methods*. The cells were then immunolabeled with an anti-Rab11 serum (middle, green) and the anti-Langerin mAb DCGM4 (right, blue). Merged images are shown in A and B. Bars, 10 $\mu$m. (C) Many BGs (arrows) are present in the cytosol, either isolated or continuous with and/or in the close vicinity of multivesicular compartments (see inset and the BGs visible in the top right-hand corner). (D) Many BGs, some of them particularly long, are also present in the perinuclear (Nu) and Golgi (G) areas. The multivesicular compartment visible in the middle on the right and indicated with a star is viewed from different angles in F. Note that the two structures (arrows) on either side of this multivesicular endosome are BGs (F, top and bottom). (E) In cells treated with both siRNA against Rab11A and chloroquine, BGs are absent from the pericentriolar area and the limiting membranes of the multivesicular compartments. Bars, 0.5 $\mu$m.

(Figure 5). This extinction was due to active lysosomal degradation, because chloroquine treatment led to the appearance of Langerin$^+$ vacuolar structures (Figure 6B, right) positive for LBPA (data not shown), a lipid particularly abundant in multivesicular and multilamellar late endosomal compartments (Gruenberg, 2003). Under the electron microscope, M10-22E cells treated with chloro-

whereas only the fuzzy top bands are still visible after 12 h of chase with (+) or without (−) chloroquine. All immunoprecipitations were carried out with lysates prepared from equivalent numbers of cells, and results shown are from one experiment representative of three independent experiments.

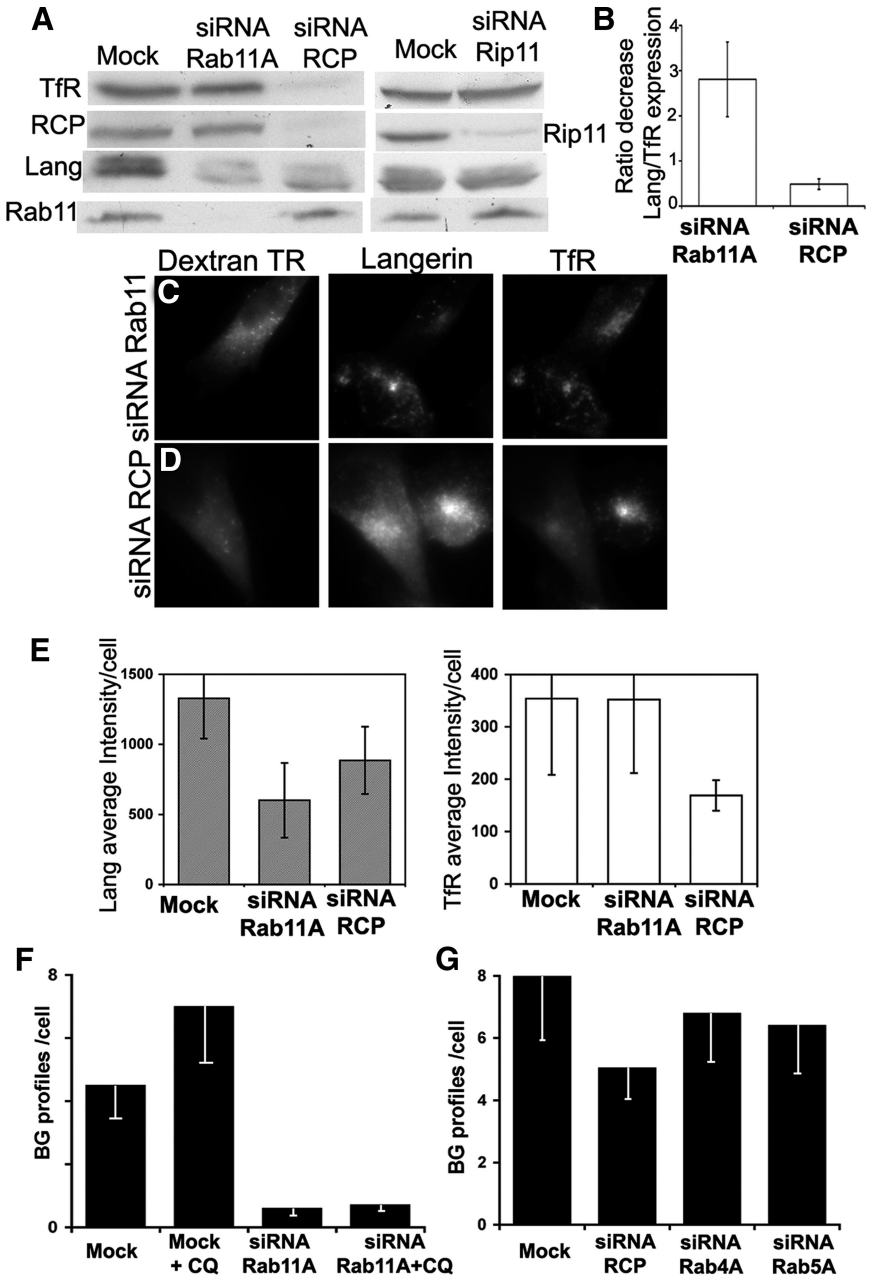


**Figure 7.** Rab11A–RCP moderately regulates Langerin stability and Birbeck granule biogenesis. (A) Immunoblotting was used to assess levels of TfR, Langerin, Rab11, RCP, and Rip11 in Langerin$^+$ HeLa cells, mock treated (mock), or treated with siRNA against Rab11A, RCP, or Rip11. The data shown are representative of five independent experiments for Rab11A and RCP siRNA and two experiments for Rip11 siRNA. Proteins were separated by SDS-PAGE in 12% acrylamide gels and blotted onto membranes. Equivalent amounts of total protein were loaded in each lane, and each blot was probed for all the proteins tested. (B) The decreases in Langerin and TfR expression were compared in cells treated with siRNA against Rab11A (5 experiments) or siRNA against RCP (5 experiments). Quantitative data derived from Western blots are presented as the ratio of the decrease in Langerin expression to the decrease in TfR expression and are normalized by the parallel results obtained in mock-treated cells (10 experiments). M10-22E cells, comicroinjected with siRNA against Rab11A (C) or siRNA against RCP (D) and Texas Red-dextran (Dextran TR, C and D, left), were immunolabeled with anti-Langerin (Langerin, C and D, middle) or anti-TfR antibodies (C and D, right) revealed with donkey anti-rabbit A488 or anti-mouse Cy5 secondary antibodies, respectively. Image stacks were acquired and the resulting immunofluorescence signals quantified (E) as described in *Materials and Methods*. Data are presented as the average fluorescence intensity (±SD) per cell for Langerin (left) and TfR (right) in cells microinjected with siRNA against Rab11A (n = 25) or RCP (n = 31) and compared with results for cells microinjected with Texas Red-dextran only (mock, n = 25). Student's *t* test was used to analyze the differences in Langerin content between cells mock treated and treated with Rab11A siRNA ($p < 0.0001$) and between cells mock treated and treated with RCP siRNA ($p = 0.015$). Quantitative analysis of the number of BG profiles per cell was performed in cells treated with Rab11A siRNA or mock treated, in the presence or absence of chloroquine (F), or in cells treated with siRNA against RCP, Rab4A, or Rab5A or mock treated (G). The number of cells examined per condition was 10 in F (but 25 for cells treated with chloroquine and siRNA against Rab11A) and 15 in G. Note the low specificity of the reduction in BG numbers in RCP-depleted cells. Only cells visible in their totality were counted, considering only sections passing through the centro-cellular region and after tilting each cell to examine it from different angles and check that no BGs had been omitted.

quine contained large numbers of BGs in the pericentriolar and Golgi areas (Figure 6, C, D, and F), where BGs are normally formed (Birbeck *et al*., 1961; Mc Dermott *et al*., 2002). These cells also contained numerous multivesicular compartments (Figure 6C, inset, and D). Occasionally, BGs seemed to be in continuity with these multivesicular structures (Figure 6C, inset). These findings contrast sharply with the ultrastructural appearance of M10-22E cells treated with both Rab11A siRNA and chloroquine, in which few BGs were found, either in the pericentriolar area or connected to the numerous multivesicular endosomes induced by chloroquine treatment (Figure 6E). A quantitative analysis confirmed the loss of BG profiles in cells treated with Rab11A siRNA (Figure 7F, siRNA Rab11A). Although chloroquine treatment increased the total number of BG profiles per cell in mock-treated cells (Figure 7F, mock + CQ), it did not reverse the effect of Rab11A siRNA (Figure 7F, siRNA Rab11A + CQ). Conversely, treatment of cells with siRNA against two other Rab proteins involved in the dynamic regulation of the endocytic recycling pathway, Rab5A and Rab4A, did not significantly modify the number of BG profiles per cell (Figure 7G). These results indicate that Langerin rescued from degradation is not able to form BGs in cells depleted of Rab11A. Thus, both Rab11A and Langerin are required for BG formation, where Rab11A plays a specific role.

### *Langerin Stability Is Partially Controlled by the RCP–Rab11A Complex*

The Rab11A dependency of BG formation may therefore depend on Langerin being present in the right membrane environment, which could be provided by Rab11–effector complexes associated with ERC membranes. Hence, we looked at the effects of two known Rab11-interacting proteins, RCP and Rip11, on the stability of Langerin and the occurrence of BGs. These two Rab11 effectors were chosen on account of the known differences in their targeted functions (Prekeris *et al*., 2000; Peden *et al*., 2004). As reported previously, the RCP knockdown induced by specific siRNA led to an almost complete extinction of TfR (Peden *et al*., 2004). Interestingly, this knockdown had only a partial effect on Langerin expression in transfected HeLa cells (Figure 7A). On the contrary, silencing of Rip11 did not significantly affect levels of either TfR or Langerin. Quantitative analysis (Figure 7B) of the relative effects of Rab11A and RCP silencing on Langerin and TfR revealed a marked difference in the behavior of these two recycling proteins, Langerin stability being tightly controlled by Rab11A and RCP expression being essential for TfR stability. Similar results were obtained in M10-22E cells (Figure 7, C–E), where quantification of fluorescence intensities demonstrated a statistically consistent decrease in Langerin expression only in cells treated with siRNA against Rab11A (Figure 7E, left graph; see legend for statistical analyses). These experiments further confirmed the strong effect of RCP silencing on TfR expression, and they supported the notion of an exclusive regulation of Langerin transport and/or stability by Rab11A rather than TfR, because no differences in the expression of the latter were detected whether the cells were treated with siRNA against Rab11A or not (mock).

As described above, ultrastructural BG profiles were counted in distinct series of M10-22E cells, mock-treated or treated with various siRNA molecules (Figure 7, F and G). Although the number of BG profiles in mock-treated cells varied with the sample preparation and their localization shifted from the ERC to multivesicular compartments, a drastic reduction in the number of BGs was always and exclusively found when the cells were silenced for Rab11A, in the presence or absence of chloroquine (Figure 6E). Silencing of RCP, which induced a partial reduction of Langerin expression (Figure 7, A and E), consistently led to a moderate decrease in the number of BGs (Figure 7G).

## DISCUSSION

In this study, we focused on the relationship between the distribution and traffic of Langerin and on the distribution and biogenesis of BGs. We tested the hypothesis that known membrane traffic regulators involved in organizing the endocytic recycling system, such as Rab proteins, might play an important role.

The production of constitutively active mutant Rab11 proteins profoundly modified the spatial organization of endosomal recycling membranes and the distribution of cargos such as Langerin and TfR. Similarly, Rab4 was found to regulate the steady-state distribution of TfR and Langerin and hence of BGs, as illustrated by the effects of the constitutively active mutant Rab4Q67L (Supplemental Figure S3, B–D). The expression of relatively small amounts of the dominant-negative mutant Rab11AS25N also resulted in a redistribution of both Langerin and TfR to tubularized recycling endosomes. However, internalized yeast invertase, which normally accumulates in $TfR^+$ $Langerin^+$ $Rab11^+$ endosomal membranes, unlike Tf, gained little access to this tubular network. One possible explanation for this apparent discrepancy is that it reflects differences in the recycling pathways taken by the two receptors. TfR returns to the plasma membrane via both a Rab11- and a Rab4-dependent pathway (Sheff *et al*., 1999), whereas Langerin recycling seems to rely more on Rab11. Therefore, the inhibition of invertase internalization in cells expressing low levels of Rab11AS25N probably results from a decrease in the rate of Langerin recycling from the ERC to the cell surface. Another hypothesis, not exclusive of the previous hypothesis, would predict that the dynamics of TfR and Langerin are controlled by different multiprotein complexes coordinated by Rab11A (Meyers and Prekeris, 2002; Peden *et al*., 2004).

One important observation is that Rab11AS25N overexpression causes the disappearance of BGs. This is of particular interest in the light of our previous observations concerning the effects of brefeldin A (BFA) on BG morphology and distribution (Mc Dermott *et al*., 2002; McDermott *et al*., 2004). BFA treatment, like Rab11AS25N overexpression, results in tubularization of the ERC in many cell types (Lippincott-Schwartz *et al*., 1991; Wilcke *et al*., 2000; Holtta-Vuori *et al*., 2002), including the cellular models used in this study (McDermott *et al*., 2004). However, BFA induces fusion of BGs with other compartments of the endocytic system, but it does not cause their disappearance. In contrast, BG formation was severely inhibited under experimental conditions where the levels of Rab11AS25N weakly affected Langerin expression, and it did not result in its exclusion from the membranes of the endosomal pathway. This strongly suggests that although Langerin can promote the formation of BGs within the ERC, the presence of an active Rab11 molecule in this compartment is also required.

This hypothesis was confirmed by using siRNAs to deplete endogenous Rab11A. Loss of Rab11A led to a strong decrease in steady-state levels of Langerin and the inhibition of yeast invertase uptake (data not shown) and BG formation. Silencing of other endocytic Rabs, including Rab4A and Rab5A, or of the Golgi/TGN-associated Rab6A/A′ did not give rise to such phenotypes, suggesting a specific involvement of Rab11A in the intracellular pathway of Langerin and the biogenesis of BGs. The inhibition of Langerin degradation by lysosomotropic agents showed that it is mistargeted to the lysosomal pathway in the absence of Rab11A or of Rab11A associated with membranes, as shown in cells overexpressing high amounts of Rab11AS25N. Importantly, even under these rescue conditions, in Rab11A-depleted cells no BGs were generated from the membranes limiting the numerous multivesicular compartments in which Langerin accumulated.

How can Rab11A control BG biogenesis? We propose that the formation of BGs depends on Langerin being addressed to an appropriate Rab11A-dependent membrane environment. In this environment, the coordinated action of Rab11A and Rab11A–effector complexes creates the membrane platform required for BG formation. In the absence of this platform, the traffic of Langerin is altered and favors its routing to lysosomal compartments where it is degraded. Because Langerin recycles actively between the endocytic system and the plasma membrane, the formation of a Rab11A-driven membrane platform must be viewed as a highly dynamic process. A defect in the membrane organization of such a platform may ultimately lead to inhibition of the biogenesis of membrane compartments such as BGs.

One previously characterized Rab11-interacting protein, RCP, could be involved in this process. RCP depletion has been shown to lead to a strong reduction of TfR expression,

which was confirmed in this study (Peden *et al*., 2004). RCP depletion also decreased Langerin levels and numbers of BGs, although to a less significant extent than in the case of TfR. As proposed for TfR, Rab11A–RCP complexes could intervene in the routing of Langerin from degradative to recycling pathways. A higher concentration of Langerin in the recycling compartments would then lead to the formation of more BGs. RCP is also known as an interconnecting protein between Rab4 and Rab11, which is suspected to link their functions in vivo (Lindsay *et al*., 2002). Although a role of RCP in the cellular organization of membranes involved in fast Rab4-dependent and slow Rab11-dependent recycling remains a matter of debate (Peden *et al*., 2004), it is tempting to correlate this notion with the present demonstration of an unequivocal Rab11A dependency of the dynamics and stability of Langerin, which is not observed for TfR. In this respect, the hypothesis that the behavior of TfR depends on Rab4–RCP and Rab11A–RCP complexes, whereas that of Langerin depends also on other distinct Rab11A complexes, could partly explain the phenotypic discrepancy between these two recycling proteins.

Given the stronger effect of Rab11A depletion compared with RCP depletion, it is likely that other Rab11A effectors are involved in BG formation. Rab11A–Rip11 complexes, at least as assessed by single knockdown of Rip11, do not seem to play a major role. Other Rab11 interacting protein candidates include the multiple proteins related to the plasma recycling system recently shown to be encoded by the *Rab11-FIP1/RCP* gene family (Jin and Goldenring, 2006). Alternatively, Langerin itself might directly associate with Rab11A–RCP and/or other Rab11A–effector complexes on BG membranes. This could be achieved by direct interaction between Rab11A and the cytoplasmic tail of Langerin, as has been described for the dimeric IgA receptor and Rab3b (van Ijzendoorn *et al*., 2002) and for the cytoplasmic domains of $\alpha$-integrin chains and Rab21 (Pellinen *et al*., 2006). However, our in vitro and in vivo biochemical investigations do not at present support this hypothesis (unpublished data).

In conclusion, this study reveals the function of Rab GTPases as membrane organizers in the endosomal pathway (Zerial and McBride, 2001). Such a role, as illustrated here for Rab11A, may lead directly or indirectly to the biogenesis of a specialized compartment. This is also supported by studies on other Rab proteins, as illustrated by the requirement of Rab5 for the integrity of early endosomes in *Drosophila* and more specifically of synaptic endosomes (Wucherpfennig *et al*., 2003).

The physiological significance of the dynamic retention of Langerin within BGs remains to be established. The BGs of LCs also contain CD1a (Hanau *et al*., 1987; Salamero *et al*., 2001), one of the group 1 CD1 proteins that present microbial lipid antigens to T cells (De Libero and Mori, 2005). Moreover, Langerin and CD1a share a common intracellular pathway in LCs, traveling through identical intracellular compartments (Salamero *et al*., 2001; Mc Dermott *et al*., 2002). Hunger *et al*. (2004) have reported that nonpeptide antigens of *Mycobacterium leprae* are presented by freshly isolated epidermal LCs to T cell clones derived from the cells of leprosy patients, in a CD1a-restricted Langerin-dependent manner. BGs may therefore correspond to a specialized membrane domain of the ERC, devoted to the loading of CD1a with glycolipids internalized and routed to the BGs by Langerin, as suggested previously by Mc Dermott *et al*. (2002).

## ACKNOWLEDGMENTS

We are especially grateful to J. Mulvihil for excellent editorial assistance, and we particularly thank Graça Raposo for technical advice and Martin Sachse for technical assistance and critical reading of the manuscript. We also thank the members of the Curie Cell and Tissue Imaging Facility for help and advice with confocal microscopy. S.U.-G. was supported by a grant from the French Ministry of Research, and D.L. was supported by the Institut National de la Santé et de la Recherche Médicale (INSERM) and Hôpitaux Universitaires de Strasbourg. This work was supported by the Association de Recherche et de Développement en Médecine et Santé Publique and the Conseil Scientifique of the Etablissement Français du Sang (EFS) (CS/2002/018) and further benefited from the continuous support of the Curie Institute, Centre National de la Recherche Scientifique, INSERM, Région Ile de France (SESAME program), and EFS-Alsace.

## REFERENCES

Agard, D. A., Hiraoka, Y., Shaw, P., and Sedat, J. (1989). Fluorescence microscopy in three dimensions. Methods Cell Biol. *30*, 353–377.

Angenieux, C. *et al*. (2005). The cellular pathway of CD1e in immature and maturing dendritic cells. Traffic *6*, 286–302.

Birbeck, M. S., Breathnach, A. S., and Everall, J. D. (1961). An electron microscope study of basal melanocytes and high-level clear cells (Langerhans cells) in vitiligo. J. Invest. Dermatol. *37*, 51–63.

Calhoun, B. C., Lapierre, L. A., Chew, C. S., and Goldenring, J. R. (1998). Rab11a redistributes to apical secretory canaliculus during stimulation of gastric parietal cells. Am. J. Physiol. *275*, C163–C170.

Chartier, C., Degryse, E., Gantzer, M., Dieterle, A., Pavirani, A., and Mehtali, M. (1996). Efficient generation of recombinant adenovirus vectors by homologous recombination in *Escherichia coli*. J. Virol. *70*, 4805–4810.

Cox, D., Lee, D. J., Dale, B. M., Calafat, J., and Greenberg, S. (2000). A Rab11-containing rapidly recycling compartment in macrophages that promotes phagocytosis. Proc. Natl. Acad. Sci. USA *97*, 680–685.

De Libero, G., and Mori, L. (2005). Recognition of lipid antigens by T cells. Nat. Rev. Immunol. *5*, 485–496.

de Renzis, S., Sonnichsen, B., and Zerial, M. (2002). Divalent Rab effectors regulate the sub-compartmental organization and sorting of early endosomes. Nat. Cell Biol. *4*, 124–133.

Del Nery, E., Miserey-Lenkei, S., Falguieres, T., Nizak, C., Johannes, L., Perez, F., and Goud, B. (2006). Rab6A and Rab6A′ GTPases play non-overlapping roles in membrane trafficking. Traffic *7*, 394–407.

Ganley, I. G., Carroll, K., Bittova, L., and Pfeffer, S. (2004). Rab9 GTPase regulates late endosome size and requires effector interaction for its stability. Mol. Biol. Cell *15*, 5420–5430.

Gruenberg, J. (2003). Lipids in endocytic membrane transport and sorting. Curr. Opin. Cell Biol. *15*, 382–388.

Hanau, D., Fabre, M., Schmitt, D. A., Stampf, J. L., Garaud, J. C., Bieber, T., Grosshans, E., Benezra, C., and Cazenave, J. P. (1987). Human epidermal Langerhans cells internalize by receptor-mediated endocytosis T6 (CD1 "NA1/34") surface antigen. Birbeck granules are involved in the intracellular traffic of the T6 antigen. J. Invest. Dermatol. *89*, 172–177.

Hanna, J., Carroll, K., and Pfeffer, S. R. (2002). Identification of residues in TIP47 essential for Rab9 binding. Proc. Natl. Acad. Sci. USA *99*, 7450–7454.

Holtta-Vuori, M., Tanhuanpaa, K., Mobius, W., Somerharju, P., and Ikonen, E. (2002). Modulation of cellular cholesterol transport and homeostasis by Rab11. Mol. Biol. Cell *13*, 3107–3122.

Hopkins, C. R., Gibson, A., Shipman, M., and Miller, K. (1990). Movement of internalized ligand-receptor complexes along a continuous endosomal reticulum. Nature *346*, 335–339.

Huang, C. C., You, J. L., Wu, M. Y., and Hsu, K. S. (2004). Rap1-induced p38 mitogen-activated protein kinase activation facilitates AMPA receptor trafficking via the GDI.Rab5 complex. Potential role in (S)-3,5-dihydroxyphenylglycene-induced long term depression. J. Biol. Chem. *279*, 12286–12292.

Hunger, R. E. *et al*. (2004). Langerhans cells utilize CD1a and Langerin to efficiently present nonpeptide antigens to T cells. J. Clin. Invest *113*, 701–708.

Imler, J. L., Chartier, C., Dreyer, D., Dieterle, A., Sainte-Marie, M., Faure, T., Pavirani, A., and Mehtali, M. (1996). Novel complementation cell lines derived from human lung carcinoma A549 cells support the growth of E1-deleted adenovirus vectors. Gene Ther. *3*, 75–84.

Jin, M., and Goldenring, J. R. (2006). The Rab11-FIP1/RCP gene codes for multiple protein transcripts related to the plasma membrane recycling system. Biochim. Biophys. Acta *1759*, 281–295.

Jordan, M., Schallhorn, A., and Wurm, F. M. (1996). Transfecting mammalian cells: optimization of critical parameters affecting calcium-phosphate precipitate formation. Nucleic Acids Res. *24*, 596–601.

Kessler, A., Tomas, E., Immler, D., Meyer, H. E., Zorzano, A., and Eckel, J. (2000). Rab11 is associated with GLUT4-containing vesicles and redistributes in response to insulin. Diabetologia *43*, 1518–1527.

Kobayashi, T., Stang, E., Fang, K. S., de Moerloose, P., Parton, R. G., and Gruenberg, J. (1998). A lipid associated with the antiphospholipid syndrome regulates endosome structure and function. Nature *392*, 193–197.

Lapierre, L. A., and Goldenring, J. R. (2005). Interactions of myosin vb with rab11 family members and cargoes traversing the plasma membrane recycling system. Methods Enzymol. *403*, 706–715.

Lindsay, A. J., Hendrick, A. G., Cantalupo, G., Senic-Matuglia, F., Goud, B., Bucci, C., and McCaffrey, M. W. (2002). Rab coupling protein (RCP), a novel Rab4 and Rab11 effector protein. J. Biol. Chem. *277*, 12190–12199.

Lippincott-Schwartz, J., Yuan, L., Tipper, C., Amherdt, M., Orci, L., and Klausner, R. D. (1991). Brefeldin A's effects on endosomes, lysosomes, and the TGN suggest a general mechanism for regulating organelle structure and membrane traffic. Cell *67*, 601–616.

Lock, J. G., and Stow, J. L. (2005). Rab11 in recycling endosomes regulates the sorting and basolateral transport of E-cadherin. Mol. Biol. Cell *16*, 1744–1755.

Martinez, O., Schmidt, A., Salamero, J., Hoflack, B., Roa, M., and Goud, B. (1994). The small GTP-binding protein rab6 functions in intra-Golgi transport. J. Cell Biol. *127*, 1575–1588.

Mc Dermott, R. *et al*. (2002). Birbeck granules are subdomains of endosomal recycling compartment in human epidermal Langerhans cells, which form where Langerin accumulates. Mol. Biol. Cell *13*, 317–335.

McDermott, R. *et al*. (2004). Reproduction of Langerin/CD207 traffic and Birbeck granule formation in a human cell line model. J. Invest. Dermatol. *123*, 72–77.

Meyers, J. M., and Prekeris, R. (2002). formation of mutually exclusive rab11 complexes with members of the family of rab11-interacting proteins regulates Rab11 endocytic targeting and function. J. Biol. Chem. *277*, 49003–49010.

Mohrmann, K., Gerez, L., Oorschot, V., Klumperman, J., and van der Sluijs, P. (2002). Rab4 function in membrane recycling from early endosomes depends on a membrane to cytoplasm cycle. J. Biol. Chem. *277*, 32029–32035.

Nedvetsky, P. I. *et al*. (2007). A role of myosin Vb and Rab11-FIP2 in the aquaporin-2 shuttle. Traffic *8*, 110–123.

Peden, A. A., Schonteich, E., Chun, J., Junutula, J. R., Scheller, R. H., and Prekeris, R. (2004). The RCP-Rab11 complex regulates endocytic protein sorting. Mol. Biol. Cell *15*, 3530–3541.

Pellinen, T., Arjonen, A., Vuoriluoto, K., Kallio, K., Fransen, J. A., and Ivaska, J. (2006). Small GTPase Rab21 regulates cell adhesion and controls endosomal traffic of beta1-integrins. J. Cell Biol. *173*, 767–780.

Pfeffer, S. (2003). Membrane domains in the secretory and endocytic pathways. Cell *112*, 507–517.

Prekeris, R., Klumperman, J., and Scheller, R. H. (2000). A Rab11/Rip11 protein complex regulates apical membrane trafficking via recycling endosomes. Mol. Cell *6*, 1437–1448.

Ren, M., Xu, G., Zeng, J., De Lemos-Chiarandini, C., Adesnik, M., and Sabatini, D. D. (1998). Hydrolysis of GTP on rab11 is required for the direct delivery of transferrin from the pericentriolar recycling compartment to the cell surface but not from sorting endosomes. Proc. Natl. Acad. Sci. USA *95*, 6187–6192.

Salamero, J., Bausinger, H., Mommaas, A. M., Lipsker, D., Proamer, F., Cazenave, J. P., Goud, B., de la Salle, H., and Hanau, D. (2001). CD1a molecules traffic through the early recycling endosomal pathway in human Langerhans cells. J. Invest. Dermatol. *116*, 401–408.

Savina, A., Fader, C. M., Damiani, M. T., and Colombo, M. I. (2005). Rab11 promotes docking and fusion of multivesicular bodies in a calcium-dependent manner. Traffic *6*, 131–143.

Savina, A., Vidal, M., and Colombo, M. I. (2002). The exosome pathway in K562 cells is regulated by Rab11. J. Cell Sci. *115*, 2505–2515.

Sheff, D. R., Daro, E. A., Hull, M., and Mellman, I. (1999). The receptor recycling pathway contains two distinct populations of early endosomes with different sorting functions. J. Cell Biol. *145*, 123–139.

Sonnichsen, B., De Renzis, S., Nielsen, E., Rietdorf, J., and Zerial, M. (2000). Distinct membrane domains on endosomes in the recycling pathway visualized by multicolor imaging of Rab4, Rab5, and Rab11. J. Cell Biol. *149*, 901–914.

Stambach, N. S., and Taylor, M. E. (2003). Characterization of carbohydrate recognition by Langerin, a C-type lectin of Langerhans cells. Glycobiology *13*, 401–410.

Ullrich, O., Reinsch, S., Urbe, S., Zerial, M., and Parton, R. G. (1996). Rab11 regulates recycling through the pericentriolar recycling endosome. J. Cell Biol. *135*, 913–924.

Valladeau, J. *et al*. (1999). The monoclonal antibody DCGM4 recognizes Langerin, a protein specific of Langerhans cells, and is rapidly internalized from the cell surface. Eur. J. Immunol. *29*, 2695–2704.

Valladeau, J. *et al*. (2000). Langerin, a novel C-type lectin specific to Langerhans cells, is an endocytic receptor that induces the formation of Birbeck granules. Immunity *12*, 71–81.

van der Sluijs, P., Hull, M., Webster, P., Male, P., Goud, B., and Mellman, I. (1992). The small GTP-binding protein rab4 controls an early sorting event on the endocytic pathway. Cell *70*, 729–740.

van Ijzendoorn, S. C., Tuvim, M. J., Weimbs, T., Dickey, B. F., and Mostov, K. E. (2002). Direct interaction between Rab3b and the polymeric immunoglobulin receptor controls ligand-stimulated transcytosis in epithelial cells. Dev. Cell *2*, 219–228.

Ward, E. S., Martinez, C., Vaccaro, C., Zhou, J., Tang, Q., and Ober, R. J. (2005). From sorting endosomes to exocytosis: association of Rab4 and Rab11 GTPases with the Fc receptor, FcRn, during recycling. Mol. Biol. Cell *16*, 2028–2038.

Westlake, C. J., Junutula, J. R., Simon, G. C., Pilli, M., Prekeris, R., Scheller, R. H., Jackson, P. K., and Eldridge, A. G. (2007). Identification of Rab11 as a small GTPase binding protein for the Evi5 oncogene. Proc. Natl. Acad. Sci. USA *104*, 1236–1241.

Wilcke, M., Johannes, L., Galli, T., Mayau, V., Goud, B., and Salamero, J. (2000). Rab11 regulates the compartmentalization of early endosomes required for efficient transport from early endosomes to the trans-Golgi network. J. Cell Biol. *151*, 1207–1220.

Wucherpfennig, T., Wilsch-Brauninger, M., and Gonzalez-Gaitan, M. (2003). Role of Drosophila Rab5 during endosomal trafficking at the synapse and evoked neurotransmitter release. J. Cell Biol. *161*, 609–624.

Zerial, M., and McBride, H. (2001). Rab proteins as membrane organizers. Nat. Rev. Mol. Cell Biol. *2*, 107–117.